


## Breakdown of heavy quasiparticles in a honeycomb Kondo lattice: A quantum Monte Carlo study

Marcin Raczkowski<sup>1</sup>,<sup>✉</sup> Bimla Danu<sup>1</sup>,<sup>✉</sup> and Fakher F. Assaad<sup>2</sup>

<sup>1</sup>*Institut für Theoretische Physik und Astrophysik, Universität Würzburg, 97074 Würzburg, Germany*

<sup>2</sup>*Institut für Theoretische Physik und Astrophysik and Würzburg-Dresden Cluster of Excellence ct.qmat, Universität Würzburg, 97074 Würzburg, Germany*

 (Received 8 July 2022; revised 13 October 2022; accepted 19 October 2022; published 31 October 2022)

We show that for the half-filled Kondo lattice model on the honeycomb lattice a Kondo breakdown occurs at small Kondo couplings  $J_k$  within the magnetically ordered phase. Our conclusions are based on auxiliary field quantum Monte Carlo simulations of the so-called composite fermion spectral function. Within a  $U(1)$  gauge theory formulation of the Kondo model, it becomes apparent that a Higgs mechanism dictates the weight of the resonance in the spectral function. For the honeycomb lattice we observe that for small  $J_k$  the quasiparticle pole gives way to incoherent spectral weight but it remains well defined for the square lattice. Our result provides an explicit example where the magnetic transition and the breakdown of heavy quasiparticles are detached as observed in  $\text{Yb}(\text{Rh}_{0.93}\text{Co}_{0.07})_2\text{Si}_2$  [S. Friedemann *et al.*, *Nat. Phys.* **5**, 465 (2009)].

DOI: [10.1103/PhysRevB.106.L161115](https://doi.org/10.1103/PhysRevB.106.L161115)

Strongly correlated many-body systems are characterized by the emergence of new elementary excitations. This can occur through the fractionalization of the electron within a parton-type construction—the fractional quantum Hall effect [1] or Luttinger liquids [2]—or through the formation of a composite object. Examples of the latter range from the understanding of single-hole dynamics in quantum antiferromagnets [3,4] to the emergence of the electron in  $\mathbb{Z}_2$  lattice gauge theories in which the electron is a bound state of an orthogonal fermion and  $\mathbb{Z}_2$  matter [5–7].

The Kondo effect is yet another example of the emergence of a composite fermion carrying the quantum numbers of the electron. Consider a spin-1/2 magnetic impurity embedded in a Fermi liquid with a finite density of states at the Fermi energy. In the presence of time reversal symmetry the Kondo coupling between the impurity and Fermi liquid is always relevant and leads to the emergence of a composite fermion. It consists of the spin-1/2 and conduction electrons and becomes itinerant, thereby releasing the  $\ln(2)$  entropy. If one replaces the metal by a Dirac liquid with a vanishing density of states at the Fermi energy, the Kondo coupling is irrelevant and one will generically observe a transition from an unscreened to screened moment at a finite value of the Kondo coupling [8,9]. This transition corresponds to the breakdown of the aforementioned composite fermion [10,11]. Such phenomena are not limited to the realm of impurity physics [12]. Neutron scattering experiments of metallic  $\text{Yb}_2\text{Pt}_2\text{Pb}$  [13] suggest a Kondo breakdown phase of a one-dimensional spin chain embedded in a three-dimensional metal. Furthermore, numerical evidence of this state of matter has been observed in models of spin chains on semimetals [14]. In dense systems such as in  $\text{YbRh}_2\text{Si}_2$  [15–17] or  $\text{CeCoIn}_5$  [18], the notion of Kondo breakdown or orbital Mott selective transitions [19] has deep implications since the composite fermions drop out from the Luttinger count. For systems with an *odd* number of localized spins per unit cell and no further spontaneous

symmetry breaking, this implies a violation of the Luttinger sum rule. Owing to Oshikawa’s [20] work such a violation can be understood if the spin system shows a topological degeneracy similar to a spin liquid [21,22]. For an *even* number of spins per unit cell, such topological constraints do not hold. In this case, Kondo breakdown does not imply a violation of Luttinger’s theorem.

Since the tight-binding model on the honeycomb lattice provides a realization of Dirac electrons, one may ask the question if and how the aforementioned Kondo breakdown transition in the impurity limit [8,9] is carried over to the dense case described by the half-filled Kondo lattice model. In Ref. [23] it is argued that the Kondo coupling is marginal in the weak-coupling limit, thereby opening the possibility of Kondo breakdown transitions in magnetically ordered metallic states. The central result of this Letter is summarized in Fig. 1: Kondo breakdown indeed occurs within the magnetic phase of the honeycomb lattice. In contrast, no breakdown is observed on the square lattice.

*U(1) gauge theory approach.* Since the Kondo effect and concomitant emergence of the composite fermion is not related to spontaneous symmetry breaking, some care has to be taken in defining the onset of these phenomena. They become particularly transparent within a  $U(1)$  gauge theory approach to the Kondo lattice model [24–26]. The Kondo lattice model (KLM) on the honeycomb lattice reads

$$\hat{H}_{\text{KLM}} = \sum_{i,j} T_{i,j} \hat{c}_i^\dagger \hat{c}_j + \frac{J_k}{2} \sum_i \hat{c}_i^\dagger \sigma \hat{c}_i \cdot \hat{S}_i, \quad (1)$$

where  $\hat{c}_i^\dagger = (\hat{c}_{i,\uparrow}^\dagger, \hat{c}_{i,\downarrow}^\dagger)$  is a spinor where  $\hat{c}_{i,\sigma}^\dagger$  creates an electron in the Wannier state centered around lattice site  $i$  and the  $z$  component of spin  $\sigma = \uparrow, \downarrow$ .  $J_k$  is the Kondo exchange coupling between conduction electrons and spins  $s = 1/2$ ,  $\hat{S}_i$ , with  $\sigma$  being a vector of Pauli spin matrices. The matrix  $T_{i,j}$  accounts for nearest-neighbor hopping with amplitude  $-t$ .

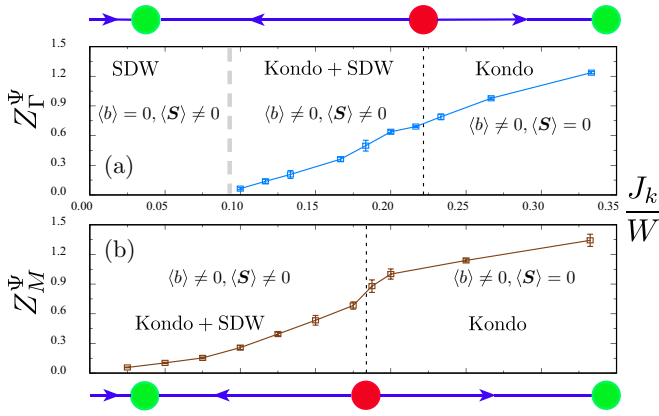


FIG. 1. Ground-state phase diagram of the half-filled Kondo lattice model on the honeycomb and square lattices. On both lattices we observe a magnetic order-disorder transition denoted by a red circle and order parameter corresponding to  $\langle S \rangle$ . For the honeycomb lattice (a) we observe a breakdown of the heavy quasiparticle in the spin-density-wave (SDW) phase as indicated by the vanishing residue  $Z_k^\psi$  of the pole at the  $\Gamma$  point in the composite fermion Green's function. For the square lattice (b) we observe only the order-disorder transition since, down to our lowest value  $J_k/W = 0.025$ ,  $Z_k^\psi$  at the  $M = (\pi, \pi)$  point remains finite. All the values of  $Z_k^\psi$  are extrapolated to the thermodynamic limit [27]. We use the mean-field notation  $\langle b \rangle$  to track the magnitude of the residue.

We adopt an Abrikosov representation of the spin operator,  $\hat{S}_i = \frac{1}{2} \hat{f}_i^\dagger \boldsymbol{\sigma} \hat{f}_i$  with  $\hat{f}_i^\dagger = (\hat{f}_{i,\uparrow}^\dagger, \hat{f}_{i,\downarrow}^\dagger)$  and constraint  $\hat{f}_i^\dagger \hat{f}_i = 1$ . To proceed we use the following rewriting of the Kondo term  $-\frac{J_k}{4} (\hat{V}_i^\dagger \hat{V}_i + \hat{V}_i \hat{V}_i^\dagger)$  with  $\hat{V}_i^\dagger = \hat{c}_i^\dagger \hat{f}_i$ . In constrained Hilbert space, this rewriting is exact. To formulate the path integral, we will work in unconstrained Hilbert space and impose it energetically with a Hubbard- $U$  term:  $H_U = U \sum_i (\hat{f}_i^\dagger \hat{f}_i - 1)^2$ . Importantly, the fermion parity on the  $f$  orbitals is a constant of motion such that it is very efficient to implement in numerical simulations. We can decouple the Kondo (Hubbard) term with a complex (real) field,  $b_i(\tau)$ ,  $a_{0,i}(\tau)$  to obtain the following action in terms of Grassmann variables  $f_i(\tau)$  and  $c_i(\tau)$ ,

$$S = S_0^c + \int_0^\beta d\tau \left\{ \sum_i \left[ \frac{2}{J_k} |b_i(\tau)|^2 + ia_{0,i}(\tau) + f_i^\dagger(\tau) \right. \right. \\ \left. \left. \times [\partial_\tau - ia_{0,i}(\tau)] f_i(\tau) + b_i(\tau) c_i^\dagger f_i + \overline{b_i(\tau)} f_i^\dagger c_i \right] \right\}, \quad (2)$$

with  $S_0^c = \int_0^\beta d\tau \sum_{i,j} c_i^\dagger(\tau) [\partial_\tau \delta_{i,j} + T_{i,j}] c_j(\tau)$ . The above corresponds to the action in the limit  $U \rightarrow \infty$  where local  $U(1)$  gauge invariance is apparent. In particular, the canonical transformation  $f_i(\tau) \rightarrow f_i(\tau) e^{i\chi_i(\tau)}$  amounts to redefining the fields  $a_{0,i}(\tau) \rightarrow a_{0,i}(\tau) + \partial_\tau \chi_i(\tau)$  and  $b_i(\tau) \rightarrow b_i(\tau) e^{-i\chi_i(\tau)}$ , such that the partition function remains invariant. We are now in a position to probe for various phases with gauge invariant quantities. Magnetism, triggered by the Ruderman-Kittel-Kasuya-Yosida (RKKY) interaction, corresponds to a spontaneous global  $SU(2)$  spin symmetry breaking and long-ranged correlations of the order parameter  $\hat{S}_i = \frac{1}{2} \hat{f}_i^\dagger \boldsymbol{\sigma} \hat{f}_i$ .

Clearly  $\hat{S}_i$  carries no  $U(1)$  charge. To define the Kondo effect we consider the fermion field

$$\tilde{f}_i(\tau) = e^{i\varphi_i(\tau)} f_i(\tau), \quad \text{with } e^{i\varphi_i(\tau)} = \frac{b_i(\tau)}{|b_i(\tau)|}. \quad (3)$$

As argued in the Supplemental Material [27],  $\tilde{f}_i(\tau)$  has the quantum numbers of a physical fermion: It carries no gauge charge, has an electron charge  $e$ , and spin  $1/2$ . The Kondo effect corresponds to the emergence of this fermion at low energies as signaled by a pole (resonance) in the dense case (single impurity limit) in the corresponding spectral function [28,29]. There is no symmetry that imposes  $\langle \tilde{f}_i(\tau) \tilde{f}_j^\dagger(\tau') \rangle$  to vanish between two space-time points and the pole in the corresponding spectral function reflects this fact. Furthermore, if the ground state turns out to be a Fermi liquid, the Luttinger volume will have to account for the composite fermion.

The above can be understood in terms of a Higgs [30] mechanism in which the phase fluctuations of  $\varphi_i(\tau)$  become very slow such that  $\varphi_i(\tau)$  can be set to a constant. In this case there is no distinction between  $\tilde{f}_i(\tau)$  and  $f_i(\tau)$  or, in other words,  $f_i(\tau)$  has lost its gauge charge and has acquired a unit electric charge. This Higgs mechanism is captured in mean-field large- $N$  approaches of the Kondo lattice where Kondo screening corresponds to  $\langle b_i(\tau) \rangle \neq 0$  [31,32].

The above definition of the fermion field  $\tilde{f}$  depends explicitly on the gauge field that is not accessible in generic numerical simulations (e.g., exact diagonalization). However, reintroducing amplitude fluctuations of the  $b$  field, we have  $\tilde{f}_i \propto b_i(\tau) f_i(\tau) \propto [f_i^\dagger(\tau) c_i(\tau)] f_i(\tau)$ . As shown in Ref. [33] and in the large- $N$  limit, the right-hand side of the latter equation is nothing but the composite fermion field,

$$\tilde{f}_i \propto \psi_i = S_i \cdot \boldsymbol{\sigma} c_i. \quad (4)$$

We also note that  $\langle b_i b_i^\dagger \rangle \propto \langle \hat{V}_i^\dagger \hat{V}_i \rangle \propto \langle \hat{c}_i^\dagger \hat{\boldsymbol{\sigma}}_i \cdot \hat{S}_i \rangle$  such that the local spin correlations between the conduction electrons and impurity spins correspond to the modulus of the boson field. If this quantity remains finite in the considered parameter regime, we will conclude that an adequate gauge field-independent representation of  $\tilde{f}_i$  is given by the composite fermion field  $\psi_i$  [34,35]. For impurity problems the Green's function of  $\hat{\psi}_i^\dagger$  corresponds to the  $T$  matrix [36] while  $\hat{\psi}_i^\dagger$  itself corresponds to the Schrieffer-Wolff transformation of the localized electron operator in the realm of the Anderson model [28].

*Method.* For our simulations we use the projective (zero-temperature) version of the algorithms for lattice fermions (ALF) [37] implementation of the auxiliary field quantum Monte Carlo (QMC) method [38–42]. For a proper comparison between honeycomb and square lattices, we set hereafter their respective tight-binding bandwidths  $W = 6t$  and  $W = 8t$  as the energy units.

*Results.* We first focus on the quantum phase transition between the magnetically ordered and disordered (Kondo) insulators and locate the phase boundary by carrying out a finite-size scaling analysis. As detailed in the Supplemental Material [27], the best data collapse gives the critical value  $J_k^c/W = 0.2227(3)$  and confirms the expected universality class of the three-dimensional classical Heisenberg  $[O(3)]$  model.

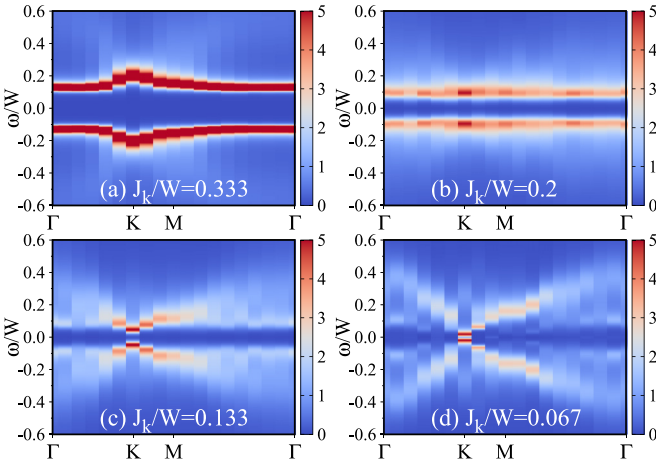


FIG. 2. Composite fermion spectral function  $A_\psi(\mathbf{k}, \omega)$  along the  $\Gamma$ - $K$ - $M$ - $\Gamma$  path in momentum space with  $\Gamma = (0, 0)$ ,  $K = (\frac{4\pi}{3}, 0)$ , and  $M = (\pi, \frac{\pi}{\sqrt{3}})$  on the  $L = 18$  honeycomb KLM for representative values of  $J_k/W$  corresponding to (a) Kondo, (b) and (c) Kondo+SDW, and (d) SDW phases.

Next, we turn to the evolution of the momentum-resolved spectral function of the composite fermion  $A_\psi(\mathbf{k}, \omega) = -\frac{1}{\pi} \text{Im} G_\psi^{\text{ret}}(\mathbf{k}, \omega)$  with  $G_\psi^{\text{ret}}(\mathbf{k}, \omega) = -i \int_0^\infty dt e^{i\omega t} \sum_\sigma \langle \{\hat{\psi}_{\mathbf{k}, \sigma}(t), \hat{\psi}_{\mathbf{k}, \sigma}^\dagger(0)\} \rangle$ . In Fig. 2(a) with  $J_k/W = 0.333$  deep in the Kondo phase, the emergent composite fermions are clearly manifest as bright weakly dispersive bands throughout the whole irreducible Brillouin zone. These bands become less pronounced upon crossing over to the magnetically ordered phase [see Figs. 2(b) and 2(c)], while some incoherent spectral weight sets in at high energies. In contrast, the spectrum in Fig. 2(d), with  $J_k/W = 0.067$  deep inside the magnetic phase, looks different: The composite fermion bands have disappeared, indicative of the breakdown of Kondo screening. If Kondo screening is not present in the magnetically ordered phase, one can adopt a large- $S$  approximation. In leading order in  $S$ , the spectral function  $A_\psi(\mathbf{k}, \omega)$  will follow the conduction electron spectral function  $A_c(\mathbf{k}, \omega)$ , i.e.,  $A_\psi(\mathbf{k}, \omega) \simeq S^2 A_c(\mathbf{k}, \omega)$  [33]. A comparison of  $A_\psi(\mathbf{k}, \omega)$  in Fig. 2(d) with the corresponding spectrum  $A_c(\mathbf{k}, \omega)$  included in the Supplemental Material [27], confirms this expectation and allows one to recognize in  $A_\psi(\mathbf{k}, \omega)$  a pronounced image of the conduction electron band consistent with the large- $S$  limit.

In order to get further insight into the observed rearrangement of spectral weight in  $A_\psi(\mathbf{k}, \omega)$ , we plot in Fig. 3(a) the raw data of  $G_\psi(\mathbf{k}, \tau)$  at the  $\Gamma$  point at our smallest Kondo coupling  $J_k/W = 0.067$  for different system sizes  $L$ . Generically, the existence of long-lived quasiparticles requires that the Green's function displays a free-particle behavior at long imaginary times,  $G(\mathbf{k}, \tau) \xrightarrow{\tau \rightarrow \infty} Z_k e^{-\Delta_{\text{qp}}(\mathbf{k})\tau}$ , where  $Z_k$  is the quasiparticle residue of the doped hole at momentum  $\mathbf{k}$  and frequency  $\omega = -\Delta_{\text{qp}}$ . As is apparent, the  $L = 6$  data quickly converge to the exponential decay, which as shown in Fig. 3(b), deceptively generates a low-energy pole, and consequently a well-defined composite fermion band, in the corresponding spectral function  $A_\psi(\mathbf{k}, \omega)$ . On the other hand, upon increasing system size it becomes more difficult to track

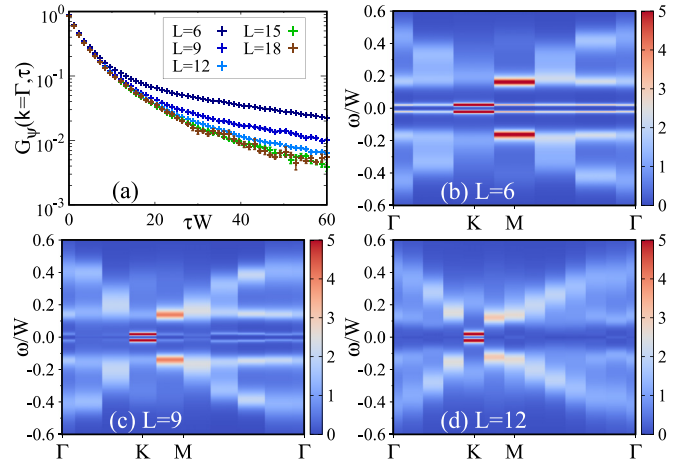


FIG. 3. (a) Composite fermion Green's function  $G_\psi(\mathbf{k} = \Gamma, \tau)$  at  $J_k/W = 0.067$ , and (b)–(d) the corresponding spectral function  $A_\psi(\mathbf{k}, \omega)$  on the honeycomb KLM with different sizes  $L$ .

the exponential form of  $G_\psi(\mathbf{k} = \Gamma, \tau)$  whose long-time tail systematically flattens. As a consequence, while a faint signature of the composite fermion band can still be spotted in  $A_\psi(\mathbf{k}, \omega)$  for  $L = 9$  [see Fig. 3(c)], the band has essentially disappeared from the  $L = 12$  spectrum in Fig. 3(d). At the same time, the overall spectrum around the  $\Gamma$  point broadens substantially and may plausibly be thought of as a continuum that stems from the decay of the composite quasiparticle. Thus, the data are suggestive of the absence of Kondo screening in the thermodynamic limit.

It is striking to compare the results in Fig. 3 with those on the square lattice obtained at an even smaller value of  $J_k/W = 0.025$  (see Fig. 4). Irrespective of the system size  $L$ , the composite fermion Green's function  $G_\psi(\mathbf{k}, \tau)$  at the  $M = (\pi, \pi)$  point shows the same asymptotic behavior in the long-time limit, which implies the continued existence of the pole in the corresponding spectrum  $A_\psi(\mathbf{k}, \omega)$  [see Figs. 4(b)–4(d)]. As can be seen,  $A_\psi(\mathbf{k}, \omega)$  shares aspects of

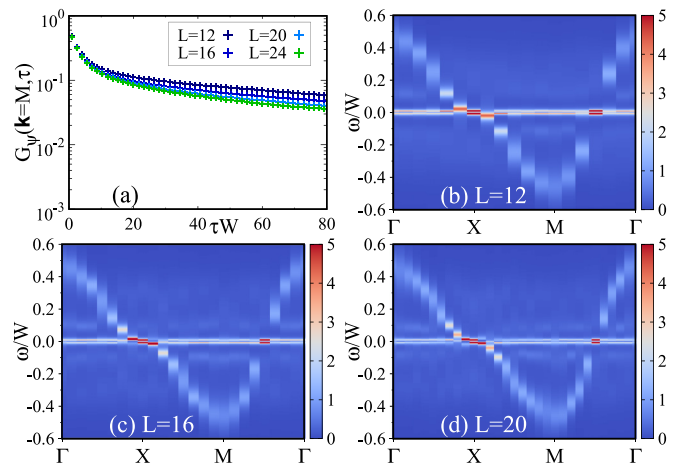


FIG. 4. (a) Composite fermion Green's function  $G_\psi(\mathbf{k} = M, \tau)$ , where  $M = (\pi, \pi)$ , at  $J_k/W = 0.025$ , and (b)–(d) the corresponding spectral function  $A_\psi(\mathbf{k}, \omega)$  along the  $\Gamma$ - $X$ - $M$ - $\Gamma$  path, where  $X = (\pi, 0)$ , on the square KLM with different sizes  $L$ .

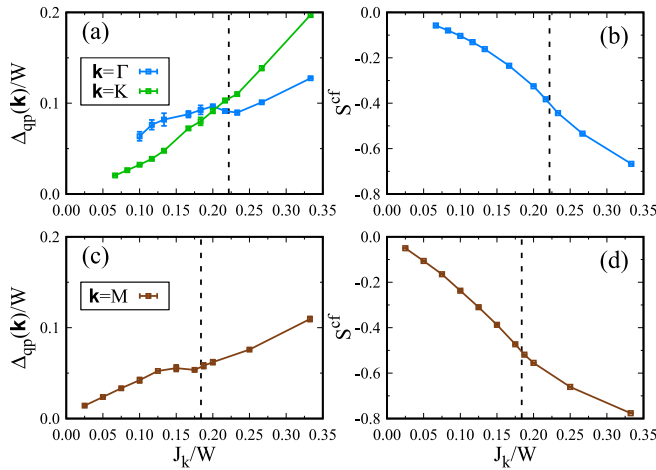


FIG. 5. (a) Single-particle gap  $\Delta_{\text{qp}}(\mathbf{k})$  at the  $\Gamma$  and Dirac  $K$  points and (b) the local spin-spin correlation function  $S^{\text{cf}}$  as a function of  $J_k/W$  on the honeycomb lattice. For comparison, we show in (c)  $\Delta_{\text{qp}}(\mathbf{k})$  at the  $M$  point and (d)  $S^{\text{cf}}$  on the square lattice. Dashed lines denote the respective magnetic order-disorder transitions. All quantities are representative of the thermodynamic limit [27].

both the large- $N$  approach (flat composite fermion bands) and large- $S$  limit, i.e., the image of the conduction electron band shifted by the antiferromagnetic wave vector  $\mathbf{Q} = (\pi, \pi)$ . Taken together, these spectral features imply the coexistence of coherent Kondo screening and long-range magnetic order.

To substantiate the vanishing of the composite fermion band as a function of  $J_k/W$ , we extract the quasiparticle residue  $Z_k^\psi$  at the  $\Gamma$  point by fitting the long-time tail of  $G_\psi(\mathbf{k} = \Gamma, \tau)$  to the exponential form followed by the finite-size scaling analysis [27]. For comparison, we have equally analyzed the asymptotic behavior of  $G_\psi(\mathbf{k}, \tau)$  at the  $M$  point on the square lattice and constructed the respective phase diagrams compiled in Fig. 1.

Since increasing  $J_k$  promotes the Kondo effect, it ultimately drives the magnetic order-disorder transition that occurs at  $J_k^c/W \simeq 0.223$  (honeycomb) and  $J_k^c/W \simeq 0.181$  (square) [43–45]. Thus, the strong-coupling region in Fig. 1 is lattice independent and hosts a Kondo screened phase. In contrast, a weak-coupling part of the phase diagram turns out to be nongeneric: While pinning down the precise scaling of  $Z_k^\psi$  at the  $\Gamma$  point on the honeycomb lattice is a challenge, our data show that it is a monotonically decreasing function of  $J_k/W$  and vanishes slightly below  $J_k/W = 0.1$ . The vanishing quasiparticle residue indicates that composite quasiparticles lose their integrity. We interpret this as the destruction of Kondo screening. This is in stark contrast to the square lattice where composite fermions are found down to our smallest value  $J_k/W = 0.025$  as signaled by a finite quasiparticle residue  $Z_k^\psi$  at the  $M$  point.

We also track the location and the size of the quasiparticle gap. Given that at large  $J_k/W$  the quasiparticle gap is located at the  $\Gamma$  point while the noninteracting model features gapless Dirac excitations at the  $K$  point, one shall resolve a change in the position of the minimal gap as a function of  $J_k/W$ . The data in Fig. 5(a) extracted from the long-time behavior of  $G_\psi(\mathbf{k}, \tau)$  at both  $\mathbf{k}$  points confirm this expectation. As is

apparent, the change takes place on the magnetically ordered side of  $J_k^c$  but far away from Kondo breakdown. Further, a comparison of Figs. 5(a) and 5(c), the latter showing the evolution of the quasiparticle gap at the  $M$  point on the square lattice, reveals two common features: (i) the development of the cusp preceding the magnetic order-disorder transition, and (ii) a linear in  $J_k/W$  scaling of the gap in the weak-coupling limit. It is a direct consequence of the Fermi-surface nesting-driven magnetic order and can be captured within a mean-field SDW framework [46,47].

Finally, as shown in Fig. 5(b) we do not resolve any signs of the breakdown of Kondo screening in the local spin-spin correlation function  $S^{\text{cf}} = \frac{2}{3N} \sum_i \langle \hat{\mathbf{c}}_i^\dagger \boldsymbol{\sigma} \hat{\mathbf{c}}_i \cdot \hat{\mathbf{S}}_i \rangle$  which remains finite down to our lowest value of  $J_k/W$ , just as that measured on the square lattice [see Fig. 5(d)]. This seemingly counter-intuitive result becomes clear by noting that  $S^{\text{cf}}$  measures the amplitude of the boson field,  $|b|^2$ . Hence, Fig. 5(b) implies that the modulus of the boson field remains constant for all values of the Kondo coupling and that Kondo breakdown occurs due to phase fluctuations. The latter explains the failure of the mean-field approaches to provide consistent results for both lattices [27].

*Summary and conclusions.* We have investigated a Kondo breakdown defined by the *destruction* of the composite fermion in Eq. (3). In the realm of the Kondo lattice considered here, this amounts to the loss of a pole in the composite fermion Green's function. Our main result is that Kondo breakdown occurs in the magnetic phase of the half-filled KLM on the honeycomb lattice. This stands in stark contrast to our results on the square lattice where down to the lowest values of the Kondo coupling, we observe no breakdown of the composite fermion. Clearly and within our numerical precision, we cannot exclude that the composite fermion residue follows an essential singularity at small  $J_k/W$  for the honeycomb geometry and a linear law for the square lattice.

Our results show that the magnetic transition and Kondo breakdown are detached as observed in  $\text{Yb}(\text{Rh}_{0.93}\text{Co}_{0.07})_2\text{Si}_2$  [48]. The observed Kondo breakdown corresponds to a modification of the excitation spectra, and does not necessarily translate into a thermodynamic transition. This stands in agreement with the Fradkin-Shenker [30] phase diagram where confined and Higgs phases are adiabatically connected. It would be of great interest to modify the KLM so as to allow for a deconfined phase and probe the full richness of the Fradkin-Shenker phase diagram as suggested in Ref. [26]. On the experimental side, we hope that our results will have an impact on the studies aimed at exploring quantum impurity problems in graphene in a dense situation [49–51].

*Acknowledgments.* We thank T. Grover and M. Vojta for many illuminating conversations and Zihong Liu for work on a related project. The authors gratefully acknowledge the Gauss Centre for Supercomputing e.V. [52] for funding this project by providing computing time on the GCS Supercomputer SUPERMUC-NG at Leibniz Supercomputing Centre [53] as well as through the John von Neumann Institute for Computing (NIC) on the GCS Supercomputer JUWELS [54] at the Jülich Supercomputing Centre (JSC). M.R. is funded by the Deutsche Forschungsgemeinschaft (DFG, German Research Foundation), Project No. 332790403. B.D. thanks

the Würzburg-Dresden Cluster of Excellence on Complexity and Topology in Quantum Matter ct.qmat (EXC 2147, project-id 390858490) for financial support. F.F.A. and B.D.

acknowledge support from the DFG funded SFB 1170 on Topological and Correlated Electronics at Surfaces and Interfaces.

- [1] J. K. Jain, Composite-Fermion Approach for the Fractional Quantum Hall Effect, *Phys. Rev. Lett.* **63**, 199 (1989).
- [2] T. Giamarchi, *Quantum Physics in One Dimension* (Oxford University Press, Oxford, U.K., 2004).
- [3] P. Béran, D. Poilblanc, and R. B. Laughlin, Evidence for composite nature of quasiparticles in the 2D  $t - J$  model, *Nucl. Phys. B* **473**, 707 (1996).
- [4] F. Grusdt, M. Kánasz-Nagy, A. Bohrdt, C. S. Chiu, G. Ji, M. Greiner, D. Greif, and E. Demler, Parton Theory of Magnetic Polarons: Mesonic Resonances and Signatures in Dynamics, *Phys. Rev. X* **8**, 011046 (2018).
- [5] R. Nandkishore, M. A. Metlitski, and T. Senthil, Orthogonal metals: The simplest non-Fermi liquids, *Phys. Rev. B* **86**, 045128 (2012).
- [6] S. Gazit, F. F. Assaad, and S. Sachdev, Fermi Surface Reconstruction without Symmetry Breaking, *Phys. Rev. X* **10**, 041057 (2020).
- [7] M. Hohenadler and F. F. Assaad, Fractionalized Metal in a Falicov-Kimball Model, *Phys. Rev. Lett.* **121**, 086601 (2018).
- [8] D. Withoff and E. Fradkin, Phase Transitions in Gapless Fermi Systems with Magnetic Impurities, *Phys. Rev. Lett.* **64**, 1835 (1990).
- [9] L. Fritz and M. Vojta, Phase transitions in the pseudogap Anderson and Kondo models: Critical dimensions, renormalization group, and local-moment criticality, *Phys. Rev. B* **70**, 214427 (2004).
- [10] Q. Si, S. Rabello, K. Ingersent, and J. L. Smith, Locally critical quantum phase transitions in strongly correlated metals, *Nature (London)* **413**, 804 (2001).
- [11] P. Coleman, C. Pépin, Q. Si, and R. Ramazashvili, How do Fermi liquids get heavy and die? *J. Phys.: Condens. Matter* **13**, R723 (2001).
- [12] A. Allerdt, A. E. Feiguin, and S. Das Sarma, Competition between Kondo effect and RKKY physics in graphene magnetism, *Phys. Rev. B* **95**, 104402 (2017).
- [13] L. S. Wu, W. J. Gannon, I. A. Zaliznyak, A. M. Tsvelik, M. Brockmann, J.-S. Caux, M. S. Kim, Y. Qiu, J. R. D. Copley, G. Ehlers, A. Podlesnyak, and M. C. Aronson, Orbital-exchange and fractional quantum number excitations in an  $f$ -electron metal, *Yb<sub>2</sub>Pt<sub>2</sub>Pb*, *Science* **352**, 1206 (2016).
- [14] B. Danu, M. Vojta, F. F. Assaad, and T. Grover, Kondo Breakdown in a Spin-1/2 Chain of Adatoms on a Dirac Semimetal, *Phys. Rev. Lett.* **125**, 206602 (2020).
- [15] S. Paschen, T. Lühmann, S. Wirth, P. Gegenwart, O. Trovarelli, C. Geibel, F. Steglich, P. Coleman, and Q. Si, Hall-effect evolution across a heavy-fermion quantum critical point, *Nature (London)* **432**, 881 (2004).
- [16] S. Friedemann, N. Oeschler, S. Wirth, C. Krellner, C. Geibel, F. Steglich, S. Paschen, S. Kirchner, and Q. Si, Fermi-surface collapse and dynamical scaling near a quantum-critical point, *Proc. Natl. Acad. Sci. U.S.A.* **107**, 14547 (2010).
- [17] L. Prochaska, X. Li, D. C. MacFarland, A. M. Andrews, M. Bonta, E. F. Bianco, S. Yazdi, W. Schrenk, H. Detz, A. Limbeck, Q. Si, E. Ringe, G. Strasser, J. Kono, and S. Paschen, Singular charge fluctuations at a magnetic quantum critical point, *Science* **367**, 285 (2020).
- [18] N. Maksimovic, D. H. Eilbott, T. Cookmeyer, F. Wan, J. Ruzs, V. Nagarajan, S. C. Haley, E. Maniv, A. Gong, S. Faubel, I. M. Hayes, A. Bangura, J. Singleton, J. C. Palmstrom, L. Winter, R. McDonald, S. Jang, P. Ai, Y. Lin, S. Cioeys, J. Gobbo, Y. Werman, P. M. Oppeneer, E. Altman, A. Lanzara, and J. G. Analytis, Evidence for a delocalization quantum phase transition without symmetry breaking in CeCoIn<sub>5</sub>, *Science* **375**, 76 (2022).
- [19] M. Vojta, Orbital-selective Mott transitions: Heavy fermions and beyond, *J. Low Temp. Phys.* **161**, 203 (2010).
- [20] M. Oshikawa, Topological Approach to Luttinger's Theorem and the Fermi Surface of a Kondo Lattice, *Phys. Rev. Lett.* **84**, 3370 (2000).
- [21] T. Senthil, S. Sachdev, and M. Vojta, Fractionalized Fermi Liquids, *Phys. Rev. Lett.* **90**, 216403 (2003).
- [22] J. S. Hofmann, F. F. Assaad, and T. Grover, Fractionalized Fermi liquid in a frustrated Kondo lattice model, *Phys. Rev. B* **100**, 035118 (2019).
- [23] S. J. Yamamoto and Q. Si, Fermi Surface and Antiferromagnetism in the Kondo Lattice: An Asymptotically Exact Solution in  $d > 1$  Dimensions, *Phys. Rev. Lett.* **99**, 016401 (2007).
- [24] N. Read and D. M. Newns, On the solution of the Coqblin-Schrieffer Hamiltonian by the large- $N$  expansion technique, *J. Phys. C: Solid State Phys.* **16**, 3273 (1983).
- [25] A. Auerbach and K. Levin, Kondo Bosons and the Kondo Lattice: Microscopic Basis for the Heavy Fermi Liquid, *Phys. Rev. Lett.* **57**, 877 (1986).
- [26] S. Saremi and P. A. Lee, Quantum critical point in the Kondo-Heisenberg model on the honeycomb lattice, *Phys. Rev. B* **75**, 165110 (2007).
- [27] See Supplemental Material at <http://link.aps.org/supplemental/10.1103/PhysRevB.106.L161115> for details of the  $U(1)$  gauge theory of the KLM, technical details of the QMC simulations, finite-size scaling analysis of the QMC data, composite fermion spectra at the  $\Gamma$  and Dirac  $K$  points, conduction electron spectral functions, as well as large- $N$  and bond fermion mean-field results, which includes Refs. [55–63].
- [28] M. Raczkowski and F. F. Assaad, Emergent Coherent Lattice Behavior in Kondo Nanosystems, *Phys. Rev. Lett.* **122**, 097203 (2019).
- [29] B. Danu, F. F. Assaad, and F. Mila, Exploring the Kondo Effect of an Extended Impurity with Chains of Co Adatoms in a Magnetic Field, *Phys. Rev. Lett.* **123**, 176601 (2019).
- [30] E. Fradkin and S. H. Shenker, Phase diagrams of lattice gauge theories with Higgs fields, *Phys. Rev. D* **19**, 3682 (1979).
- [31] S. Burdin, A. Georges, and D. R. Grempel, Coherence Scale of the Kondo Lattice, *Phys. Rev. Lett.* **85**, 1048 (2000).
- [32] D. K. Morr, Theory of scanning tunneling spectroscopy: From Kondo impurities to heavy fermion materials, *Rep. Prog. Phys.* **80**, 014502 (2017).

- [33] B. Danu, Z. Liu, F. F. Assaad, and M. Raczkowski, Zooming in on heavy fermions in Kondo lattice models, *Phys. Rev. B* **104**, 155128 (2021).
- [34] T. A. Costi, Kondo Effect in a Magnetic Field and the Magnetoresistivity of Kondo Alloys, *Phys. Rev. Lett.* **85**, 1504 (2000).
- [35] M. Maltseva, M. Dzero, and P. Coleman, Electron Cotunneling into a Kondo Lattice, *Phys. Rev. Lett.* **103**, 206402 (2009).
- [36] L. Borda, L. Fritz, N. Andrei, and G. Zaránd, Theory of inelastic scattering from quantum impurities, *Phys. Rev. B* **75**, 235112 (2007).
- [37] F. F. Assaad, M. Bercx, F. Goth, A. Götz, J. S. Hofmann, E. Huffman, Z. Liu, F. P. Toldin, J. S. E. Portela, and J. Schwab, The ALF (Algorithms for Lattice Fermions) project release 2.0. Documentation for the auxiliary-field quantum Monte Carlo code, *SciPost Phys. Codebases*, **1** (2022).
- [38] R. Blankenbecler, D. J. Scalapino, and R. L. Sugar, Monte Carlo calculations of coupled boson-fermion systems. I, *Phys. Rev. D* **24**, 2278 (1981).
- [39] G. Sugiyama and S. Koonin, Auxiliary field Monte-Carlo for quantum many-body ground states, *Ann. Phys.* **168**, 1 (1986).
- [40] S. R. White, D. J. Scalapino, R. L. Sugar, E. Y. Loh, J. E. Gubernatis, and R. T. Scalettar, Numerical study of the two-dimensional Hubbard model, *Phys. Rev. B* **40**, 506 (1989).
- [41] S. Sorella, S. Baroni, R. Car, and M. Parrinello, A novel technique for the simulation of interacting fermion systems, *Europhys. Lett.* **8**, 663 (1989).
- [42] F. F. Assaad and H. Evertz, in *Computational Many-Particle Physics*, edited by H. Fehske, R. Schneider, and A. Weiße, Lecture Notes in Physics, Vol. 739 (Springer, Berlin, 2008), pp. 277–356.
- [43] F. F. Assaad, Quantum Monte Carlo Simulations of the Half-Filled Two-Dimensional Kondo Lattice Model, *Phys. Rev. Lett.* **83**, 796 (1999).
- [44] S. Capponi and F. F. Assaad, Spin and charge dynamics of the ferromagnetic and antiferromagnetic two-dimensional half-filled Kondo lattice model, *Phys. Rev. B* **63**, 155114 (2001).
- [45] M. Raczkowski and F. F. Assaad, Phase diagram and dynamics of the  $SU(N)$  symmetric Kondo lattice model, *Phys. Rev. Res.* **2**, 013276 (2020).
- [46] Y. Zhong, K. Liu, W. Yu-Feng, Y.-Q. Wang, and H.-G. Luo, Half-filled Kondo lattice on the honeycomb lattice, *Eur. Phys. J. B* **86**, 195 (2013).
- [47] G.-M. Zhang and L. Yu, Kondo singlet state coexisting with antiferromagnetic long-range order: A possible ground state for Kondo insulators, *Phys. Rev. B* **62**, 76 (2000).
- [48] S. Friedemann, T. Westerkamp, M. Brando, N. Oeschler, S. Wirth, P. Gegenwart, C. Krellner, C. Geibel, and F. Steglich, Detaching the antiferromagnetic quantum critical point from the Fermi-surface reconstruction in  $\text{YbRh}_2\text{Si}_2$ , *Nat. Phys.* **5**, 465 (2009).
- [49] L. Fritz and M. Vojta, The physics of Kondo impurities in graphene, *Rep. Prog. Phys.* **76**, 032501 (2013).
- [50] Y. Jiang, P.-W. Lo, D. May, G. Li, G.-Y. Guo, F. B. Anders, T. Taniguchi, K. Watanabe, J. Mao, and E. Y. Andrei, Inducing Kondo screening of vacancy magnetic moments in graphene with gating and local curvature, *Nat. Commun.* **9**, 2349 (2018).
- [51] J. Hwang, K. Kim, H. Ryu, J. Kim, J.-E. Lee, S. Kim, M. Kang, B.-G. Park, A. Lanzara, J. Chung, S.-K. Mo, J. Denlinger, B. I. Min, and C. Hwang, Emergence of Kondo resonance in graphene intercalated with Cerium, *Nano Lett.* **18**, 3661 (2018).
- [52] [www.gauss-centre.eu](http://www.gauss-centre.eu)
- [53] [www.lrz.de](http://www.lrz.de)
- [54] Jülich Supercomputing Centre, JUWELS: Modular Tier-0/1 Supercomputer at the Jülich Supercomputing Centre, *J. Large-Scale Res. Facil.* **5**, A135 (2019).
- [55] J. W. Negele and H. Orland, *Quantum Many-Particle Systems* (Westview Press, Boulder, CO, 1998).
- [56] T. Hazra and P. Coleman, Luttinger sum rules and spin fractionalization in the  $SU(N)$  Kondo lattice, *Phys. Rev. Res.* **3**, 033284 (2021).
- [57] C. Wu and S.-C. Zhang, Sufficient condition for absence of the sign problem in the fermionic quantum Monte Carlo algorithm, *Phys. Rev. B* **71**, 155115 (2005).
- [58] T. Sato, F. F. Assaad, and T. Grover, Quantum Monte Carlo Simulation of Frustrated Kondo Lattice Models, *Phys. Rev. Lett.* **120**, 107201 (2018).
- [59] K. S. D. Beach, Identifying the maximum entropy method as a special limit of stochastic analytic continuation, [arXiv:cond-mat/0403055](https://arxiv.org/abs/cond-mat/0403055).
- [60] S. M. Chester, W. Landry, J. Liu, D. Poland, D. Simmons-Duffin, N. Su, and A. Vichi, Bootstrapping Heisenberg magnets and their cubic instability, *Phys. Rev. D* **104**, 105013 (2021).
- [61] H. Watanabe and M. Ogata, Fermi-Surface Reconstruction without Breakdown of Kondo Screening at the Quantum Critical Point, *Phys. Rev. Lett.* **99**, 136401 (2007).
- [62] C. Jurecka and W. Brenig, Bond-operator mean-field theory of the half-filled Kondo lattice model, *Phys. Rev. B* **64**, 092406 (2001).
- [63] R. Eder and P. Wróbel, Antiferromagnetic phase of the Kondo insulator, *Phys. Rev. B* **98**, 245125 (2018).